Theoretical study on Slotted Photonic Crystal Cavity for Sensing

AHLEM BENMERKH, TOURAYA BOUCHEMAT, MOHAMED BOUCHEMAT

University Frères Mentouri, Electronics Department,
Constantine 1, ALGERIA

Abstract. The objective of this work has been a proposition of the refractive index sensor design based on slotted L_2 photonic crystal cavity with a triangular lattice of air holes patterned perpendicularly to an InP-based confining heterostructure. Three slots located into the cavity and the two rows of functionnalized holes nearby the resonant cavities are totally injected with analyte. The quality factor of biosensor is over 3.4677 10^7, and the sensitivity is obtained as 440 nm/RIU for the optimized structure. Our results propose a refractive index detection limit is about $9.56x10^{-8}$ RIU.
Keywords: Photonics, Crystal Cavities, Sensing

1 Introduction

In order to meet the rising demand for health and environmental analyzes and the need for medical diagnosis ever faster and more reliable, research activities on biological or chemical sensors of new generation are becoming more intense. In particular, optical devices integrated on chip offering a high potential for the development of generic transducers, compatible with the parallel detection without markers of a wide variety of biomolecules and a spectral range that can be adjusted from visible to infrared where the absorption of many materials and biological noise are greatly reduced [1]. In this context, a new way to nanotechnologies: photonic crystal biosensors, has been explored.

The refractive slotted with guides were initially proposed by Almeida et al. in 2004 [2]. The authors showed that by exploiting the total internal reflection condition (TIR) in a waveguide, it was possible confining the field in the low index material within a slot and forming a guide with a planar hollow core when this method is used. Depending on the width of the slot, it is possible to confine up to 30% the total power of the fundamental mode. The very strong electric field intensity in the hollow core of the guide is of great interest for photonic applications. First, it allows building high sensitivity sensors unlike many sensors based on silicon photonic structures; the detected material (nanoparticles, gas, proteins...) interacts directly with the confined field and not its evanescent part. Another application of great interest lies in the field of nonlinear optics and amplification. It is indeed possible to infiltrate the slot by materials with a very high Kerr coefficient, of direct electro-optic effect (Pockels) or the stimulated emission properties. These applications were the subject of abundant literature and made slot guides a promising hybrid platform for optical information processing.

The first proposed confinement of the optical mode in a microcavity with a slot was made by Robinson et al. [3]. The authors's work has shown that modal volumes of dimensions very smaller than the wavelength by exploiting the strong discontinuity of the field to the dielectric/air interface can be achieved. The first study of slotted photonic crystal cavity consisted of inserting a slot in a cavity type A1. The strategy to bring the cavity field maxima in free space is to introduce a narrow longitudinal air slot onto the center of the width-modulated line-defect cavities that have ultrahigh Q over one million [4]. In another work, Wülbern et al. have proposed a concept using a double heterostructure cavity in a slotted silicon PhC waveguide, infiltrated with nonlinear optical polymer to operate as an electro-optic modulator [5]. The next sensor is based on Ln (n>3) slot microcavity, which operate as refractive index (RI) gas sensors. The authors experimentally demonstrated an L9 slot microcavity with Q exceeding 3 10^4, S =421 nm/RIU, and DL= 1 $x10^{-5}$ RIU which is the best result for non-heterostructure PC sensors [6]. The advantage of the slot PC cavities is that they are characterized by modal volumes that can be up to two orders of magnitude lower than conventional cavities for relatively high quality factors. .

In this paper, we propose a slotted photonic crystal microcavity with triangular lattice of air holes, the slots into the cavity are totally injected with analyte. In this structure, we are interested on the design and optimization of the PC cavity to realize higher Q factor

and larger sensitivity. For that we act on several parameters such as width and length of the slot and the number of functionalized holes (N) nearby the resonant cavities in the photonic crystal sensor. We have achieved for the optimised structure the maximum Q factor as large as 3.4677 10^7 appears at 1.46µm while the sensitivity keeps a relatively high value of 440 nm/RIU when the refractive index is 1.33. The calculated detect limit lower than 9.56 x10^{-8} RIU is obtained.

2 Design of the PC slot microcavity

In the designed structure shown in Fig. 1, 2D triangular PC of air holes patterned perpendicularly to an InP-based confining. The planar guide that is a core heterostructure GaInAsP (refractive index 3.35) of thickness 1.00a. The core is surrounded by two cladding InP (refractive index 3.17) of thickness 0.50a. The lattice constant is a = 440 nm while the hole radius is r = 0.4a. This gives an effective index of 3.32 for the fundamental TE guided mode. It depends on the polarization of light and takes into account the third dimension in that light encounters an average index between the core and the cladding. This approximation dramatically reduces the computation time necessary for full 3D calculations and is generally quite useful as a guide is determining the fundamental bandgap frequency and lowerlying frequency band dispersion curves.

The structure is simulated by plane wave expansion (PWE) and has a photonic bandgap (PBG) for transverse-electric modes, which have no electric field in the direction of propagation. The PBG extends from 0.2564 (a/ λ) to 0.4507 (a/ λ), where λ is the wavelength of light in free space.

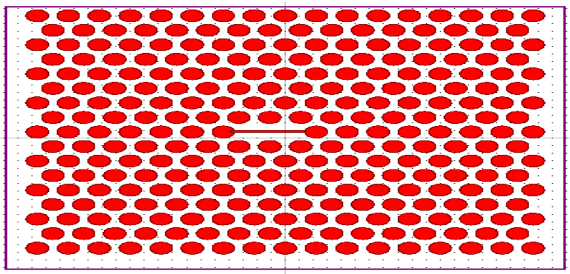

Fig. 1. The schematic diagram of an air-slot microcavity confined with mode gap created in a 2D triangular-lattice photonic crystal.

In order to increase the Q factor and reduce the mode area, we propose an air slot-photonic crystal cavity. Fig. 1b shows the schematic diagram of the designed air-slot PC cavity (SPCC). First, a linear cavity (L2 cavity) is created by removing two holes in the center.

Rectangular slot with cross-sectional dimensions of $W_X \times W_Y$ is introduced into the center of L_2 cavity. The symbol W_X and W_Y represent the slot length along the x and y axes, respectively. The computational method used is based on a 2D finite difference time domain (FDTD) method algorithm. Perfectly matched layers conditions have been considered in the calculations to ensure no back reflection in the limit of the analyzed region [7]. This crystal is lit by a Gaussian wave under normal incidence with a transverse electric (TE) polarized mode. The length of the photonic crystal is 17a and the time step is chosen to 0.01. Note that it might be necessary to reduce the time step below the stability limit when simulating metals since the courant condition can change in this case.

The Q factor is defined as $\lambda_0/\Delta\lambda$, where $\Delta\lambda$ is the FWHM of the resonator's Lorentzian response and λ_0 is the resonance wavelength. In this case the automated Q-finder tool calculates the Q factor using 2D finite-difference time-domain (FDTD) method, combined with fast harmonic analysis techniques [7].

We found the L_2 microcavity without slot has the resonance mode located at λ= 1.5285 µm where the Q factor calculated at this resonance is about 2.1408 10^6.

Slot photonic crystal in InP heterostructure holes have been studies by several papers [8]. Examples of such structures contain the work of K. Cui et al. [8] fabricated the double slot PC waveguide by inductively coupled plasma (ICP) etching. The promising experimental results evidence the high etching quality and confirm the feasibility of etching small-feature-size patterns by ICP technology for InP based devices in future mono-/hetero-integrated photonic circuits.

The slotted L_2 cavity consists, as its name implies, an air slot inserted into the L_2 cavity (see Fig.1b). Based on this structure, the transmission spectrum of an air SPCC is shown in Fig. 2, $(W_Y = 40nm,\ W_X = 700nm)$ and the results display obviously a resonant mode located at 1.4986µm. This mode has a quality factor of 4.4 10^7. It is found that the resonant wavelength of the SPCC shift gets smaller because this cavity behaves in the same manner of L_2 cavity (without slot) by moving the holes adjacent the cavity. The effective refractive index in the cavity region is reduced by the slots, which shifts the cavity resonance away from the bandgap.

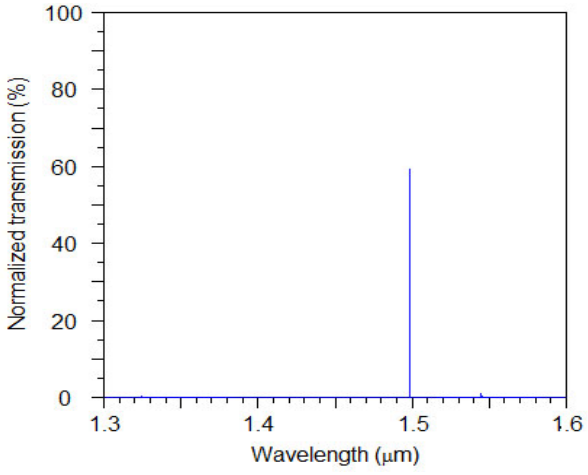

Fig.2: Transmission spectrum of the air-slot PC cavity in a triangular lattice.

To estimate the functionality of the structure, a sample, for example the water, where the liquid with low refractive index can be infiltrated into the slot. The possibility of filling the through etched slot waveguides with different ambient refractive indexes was fabricated by some researchers, more details of which can be found in [6], [9-11].

For sensor applications, not only the quality factor is crucial to gain high sensitivity, but also the intensity is related to the number of photons, and makes no sense for individual photons. For that we act on several parameters such as width and length of the slot and the number of functionalized holes (N) nearby the resonant cavities in the photonic crystal sensor.

In order to discuss the sensing performances of the proposed 2D SPCC influenced by the width and length of the slot, numerical 2D-FDTD simulations are calculated. The transmission spectrum obtained by this cavity is represented in figure 3a and 3c.

Fig. 3b and 3d illustrates the simulation results for the resonant wavelength and Q values of the cavity with different slot widths and lengths.

First, we fix the length of the slot at 1100 nm and the slot width varies from 30 nm to 80 nm. When the liquid-slot width broadens, the resonant wavelength will decreases linearly from 1.5379 to 1.4042 µm and Q values can be tuned from 1.83 10^7 to 3.5011 10^7, which are shown in Fig. 3b. Note that the maximum Q value of for the water-slot cavity can be achieved when the water-slot width are 60nm. In other words, the Q value of the cavity will diminish no matter the slot width becomes larger or smaller than 60 nm. Because the optical mode is more localized with the increase of slot width when the width of slot is less than 60nm, and the photon life time can be enhanced and the higher Q factor can be achieved, whereas it turns to the contrary tendency when the width of slot is more than 60nm. With the width of slot increased, the high dielectric material is decreased and the low-dielectric material is increased in the cavity region, as a result, the resonance frequencies is pushed to higher frequency (lower wavelength). In addition, the variation of optical properties is very sensitive to the water-slot width, and fine adjustment can be realized.

As can be seen, the maximum Q factor as large as 3.50 10^7 appears at $W_Y = 60nm$ at the resonant mode located at 1.4385µm but the transmission is very low (see Fig. 3a and 3b). So, we choose the Q factor of 2.2283 10^7 at the resonant mode located at 1.5194 µm with $W_Y = 40nm$ as the optimum result due to its high Q factor, and high transmission simultaneously.

Changing the slot length (W_x) also affects the Q factor and resonant wavelength. We fix $W_Y = 40nm$ and adjust W_x. The transmission curve determination for different lengths as, described in Fig. 3c, gives the best slot length founding ($W_X = 700nm$) due to its relatively high transmission and Q factor. Then the calculated Q-factor value for the resonant mode located at 1.5613µm for $W_X = 700nm$ was above 1.5183 10^7 (see Fig.3d).

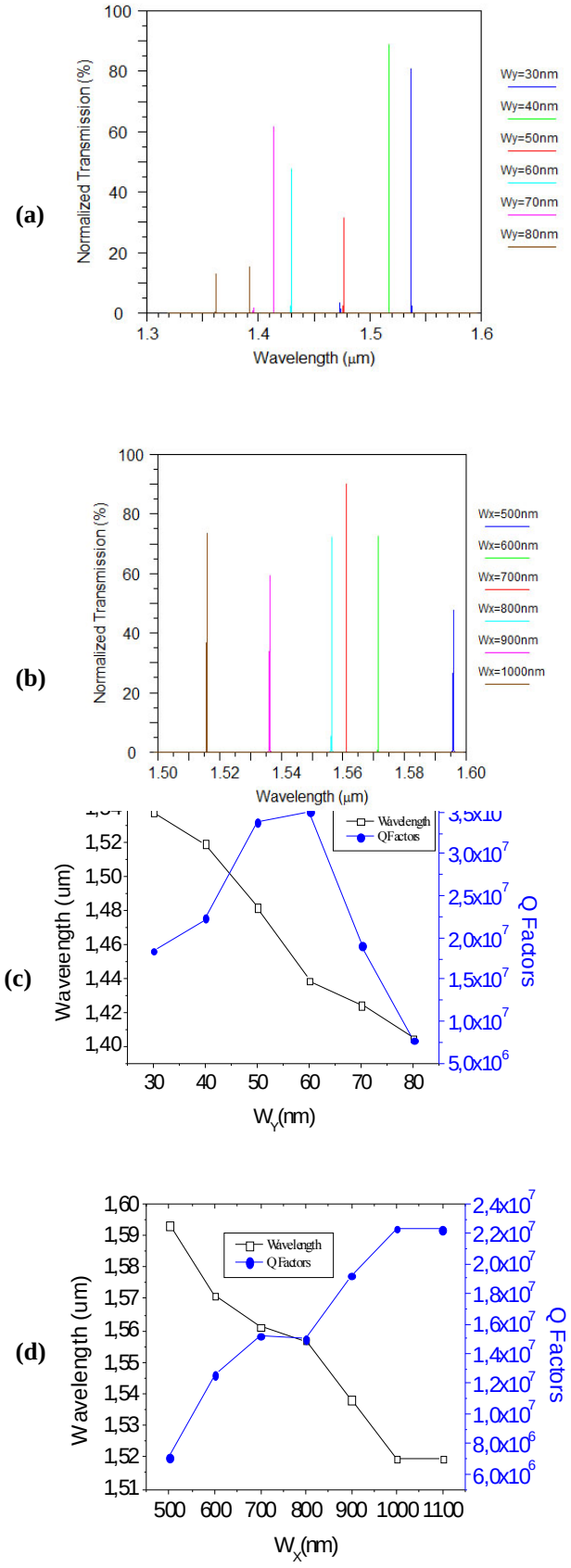

Fig.3: The transmission spectra of TE polarized light-wave with different values of (a) widths and (c) Lengths, Quality factor and wavelength mode as a function of the (b) widths (Wx) and (d) Lengths (Wy).

Based on the above optimal design $(W_Y = 40nm,\ W_X = 700nm)$, it is essential to note that the magnitude of the resonant wavelength shift is dependent on the combination of many factors such as the number of the slot inside the cavity (M) and the number of the functionalized holes (N) around the SPCC change. We assume that the slots are totally injected with analyte.

Here, we try different number of slots inside the cavities of the photonic crystal sensor illustrated in Fig. 4. The transmission curve determination for different (M) as, described in Fig. 5a. As seen in this figure, the resonant wavelength of the microcavity shift gets smaller as the number of slots increases due to the effective index in the cavity region is reduced by the slots.

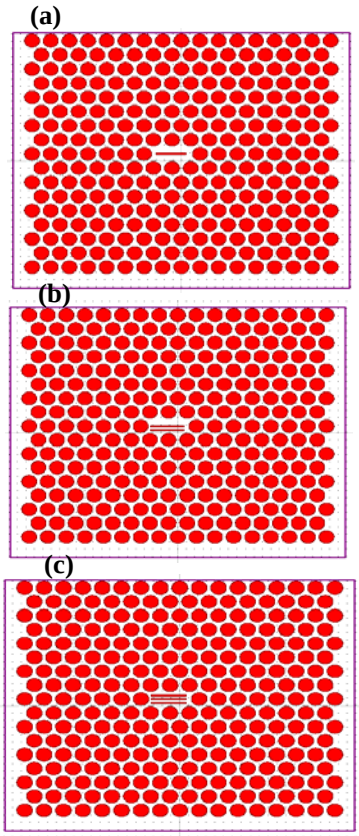

Fig.4: Schematic of the slotted photonic crystal cavity: (a) one slot, (b) two slots and (c) three slots.

As can be seen, the maximum Q factor, as large as 9.72 × 10^7, is obtained for M=3 at the mode resonant located at 1.4123 µm (see fig.5b). Thus, we choose this value as the optimum result due to its high transmission and Q factor simultaneously. It is observed that the number of the slots inside the L_2 cavity are greatly affects on the position and the quality factor of the resonant mode. Some researchers have design, fabricate, and characterize the SPCC structure with three slots are placed in a silicon photonic crystal slab where three holes are removed. The theoritecal Q factor above 60000, in which the linear defect was expanted to $W_{1.35}$ [12]. The intensity field distribution of the resonant mode located at λ= 1.4123 µm for the slotted L_2 cavity is represented in Fig. 5c.

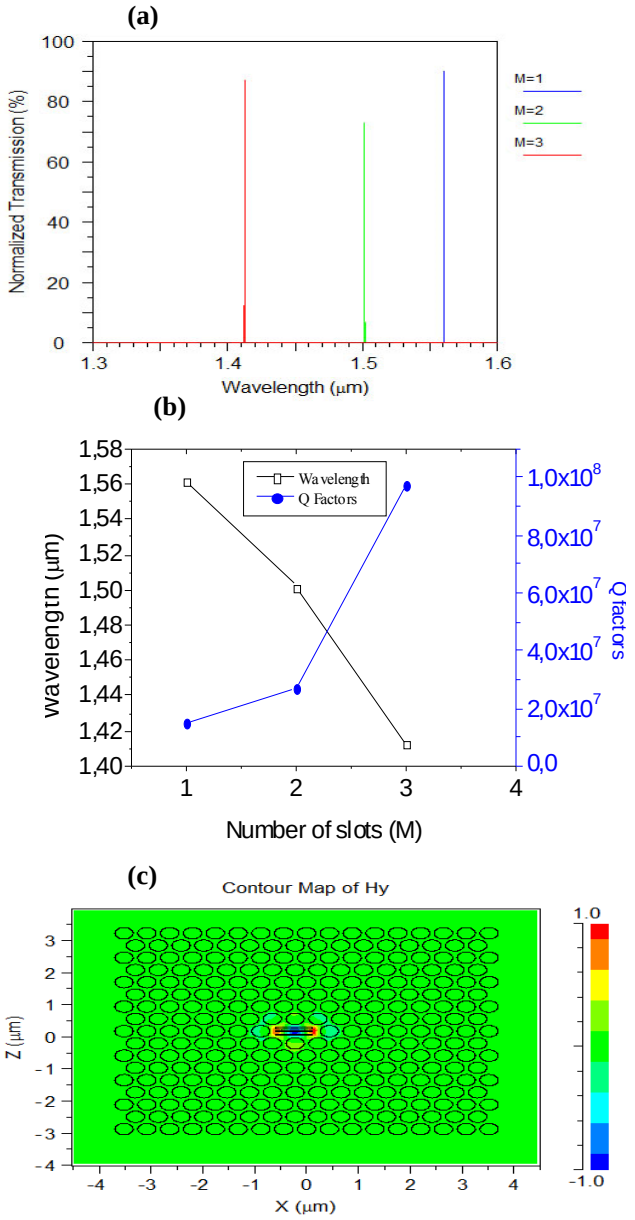

Fig.5: (a) Calculated transmission spectra of the sensor for different number of the slot inside the cavity (M), (b) Quality factor and wavelength mode as a function of the number of the slot inside the cavity (M) and (c) The intensity field distribution for the mode with three slots inside the cavity at λ=1.4123 µm.

Next, we studied the sensing performance of the designed sensor (M=1, 2, 3) in ambient refractive index sensing, the simulation results under different slot refractive indices are analyzed. Fig. 6 shows the resonant wavelength of the L_2 slot microcavity under different refractive index of the infiltrated liquid increases from 1.33 to 1.36 with the interval of 0.005 when the slot width and length are respectively is 40 and 700 nm.

Based in this linear relationship, we obseved for one slot inside the cavity (M=1) the resonance wavelength shift is approximately 0.75 nm and the calculated RI sensitivities ($S = \Delta\lambda/\Delta n$) of this sensor S=150 nm/RIU. Taking water absorption into consideration a telecom wavelength range, the Q factor is equal to 1.5183 10^7 ($Q_{1.33}$). Then for two slots (M=2), we obtain a shift in wavelength of 0.9 nm, equivalent to the sensitivity of 180 nm/RIU with the Q factor as large as 2.6994 10^7($Q_{1.33}$). In the next design where three slots are introduced into the cavity (M=3). The cavity gives a shift of 1.4 nm, equivalent to the sensitivity of 280 nm/RIU and a quality factor of 9.7289 10^7 is obtained. We found that the SPCC with three slots has a larger wavelength shift than the one and two slots. In other words, it has a higher refractive index sensitivity that is due to the reduced refractive index difference between the holes and the semiconductor membrane. Hence, for sensing applications, it is desirable to design a device that has a large resonance frequency change for small variation of refractive index in the slots.

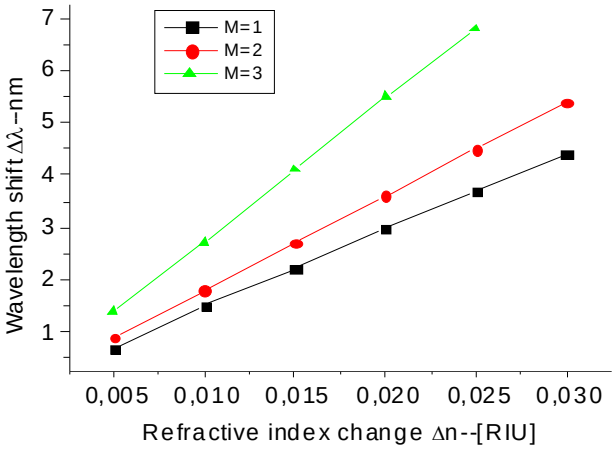

Fig.6. Resonant wavelength shifts as a function of refractive index change of slots.

After that, we take the optimal structure with three slots. We try different number of functionalized holes (N) nearby the resonant cavities in the photonic crystal sensor with three slots illustrated in Fig. 7 (indicated by the blue circular holes) to study the relationship between the sensitivity and the number of functionalized holes. The holes surrounding the cavity are locally filled with liquids has been demonstrated experimentally in [13-15], a novel lithographic technique of tuning PC devices, based on local mask opening for individual holes. This enables the use of any post production method on the exposed area of the PC, while not affecting other holes in the PC [13].

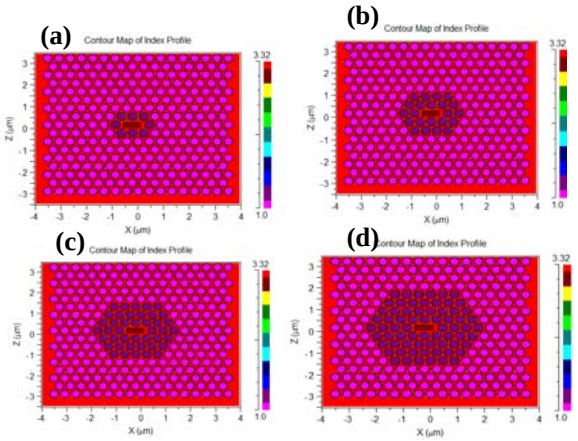

Fig.7: The computed index profile of the L_2 cavity filled with polymer made by removed two holes.

The transmission curve determination for different functionalized holes (N) as, described in Fig. 8a. As seen in this figure, the resonant wavelength of the microcavity shift gets larger (the sensitivity becomes higher) as the number of functionalized holes increases due to the reduced refractive index difference between the holes and the semiconductor membrane [16]. It can be noted that when the number of functionalized holes increases, the resonance quality factor decrease due to the reduced refractive index difference between the holes and the semiconductor membrane, and thus to the reduced reflectivity of the PC boundaries because of the weaker vertical confinement that increases the out-of-plain losses (see Fig.8b).

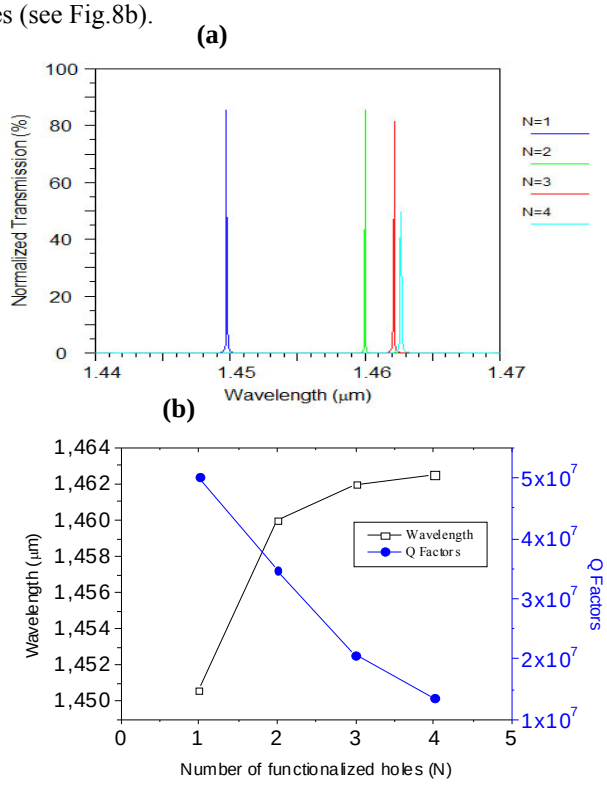

Fig.8. (a) Transmission spectra with different number of functionalized circular holes (N) and (b) Quality factor and wavelength mode as a function of the number of functionalized circular holes (N).

To investigate the sensitivity of the SPCC sensor arrays, we perform a series of simulations under different refractive index for different functionalized holes (N=1, 2, 3, 4). According to the simulation results, we obtain the sensitivity shown in Fig. 9. As seen in this figure, the resonant wavelength shift gets larger as the number of functionalized holes (N) increases from one row (N=1) to two rows (N=2) while for N greater than two the wavelength shift slightly.

So we could choose the resonant mode located at 1.46 µm with (N =2) as the optimum result due to its relatively high sensitivity, high-Q factor and high transmission. This cavity gives a shift of 2.2 nm, equivalent to the sensitivity of 440 nm/RIU and a quality factor of 3.4677 10^7 is obtained. In comparison with other PC cavity-based refractive index sensor [6, 17], our designed sensor has higher sensitivity and Q factor simultaneously.

High sensor performance requires a low detection limit (DL), which is inversely proportional to Q and S. The detection limit of refractive index change is further researched which could be defined as [18]:

$$DL = \frac{\lambda}{SQ}$$

Where λ is the resonant wavelength, S represents the refractive index sensitivity, and Q means the quality factor. Then numerical simulations show that the detection limit of refractive index change is about $9.56x10^{-8}$ RIU, which is well optimized than the previous design [6].

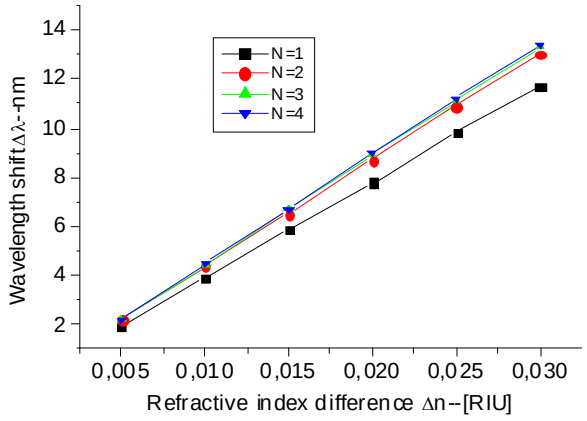

Fig.9. Resonant wavelength shifts as a function of refractive index change of fictionalized holes.

3 Conclusion

In summary, We have presented a refractive index sensor based on slotted photonic crystal cavity where the three slots in the center of the cavity and the functionnalized holes are infiltrated with water. With 2D-FDTD simulations, high sensitivity as 440 nm/RIU and high quality-factor as 3.4677 10^7 are achieved simultaneously. The calculated detect limit lower than $9.56x10^{-8}$ RIU is obtained.

Acknowledgement

The authors would like to thank professor Mohamed Benidir for his help.

References

[1] T. Benyattou, "Biocapteurs à cristaux photoniques sur silicium," Ecole doctorale EEA de Lyon.

[2] V. R. Almeida, Q. Xu, C. A. Barrios, M. Lipson, Optics Letters **29**, 1209 (2004).

[3] J. T. Robinson, C. Manolatou, L. Chen, M. Lipson, Physical Review Letters **95**, 143905 (2005).

[4] T. Yamamoto, M. Notomi, H. Taniyama, E. Kuramochi, Y. Yoshikawa, Y. Torii, T. Kuga, Optics Express **16**, 13809 (2008).

[5] J.-H. Wülbern, J. Hampe, A. Petrov, M. Eich, J. Luo, A. K.-Y. Jen, A. Di Falco, T. F. Krauss, J. Bruns, Applied Physics Letters **94**, 241107 (2009).

[6] K. Li, J. Li, Y. Song, G. Fang, C. Li, Z. Feng, R. Su, B. Zeng, X. Wang, and C. Jin, IEEE photonics Journal **6**, 1-9 (2014).

[7] The FDTD simulations were carried out with Fullwave commercial software byRSoft Design Group, version 6.1, license 16847214.7.

[8] K. Cui, Y. Li, X. Feng, Y. Huang, and W. Zhang, AIP Advances **3**, 022122-1-8 (2013).

[9] Kristinn B. Gylfason, "Integrated Optical Slot-Waveguide Ring Resonator Sensor Arrays for Lab-on-Chip Applications," Thesis, School of Electrical Engineering, 2010.

[10] M. G. Scullion, T. F. Krauss and Andrea Di Falco, Sensors **13**, 3675-3710 (2013).

[11] Y. Liu, and H.W.M Salemink, Appl. Phys.Lett.**106**, 031116-1 (2015).

[12] J. Zheng, X. Sun, Y. Li, M. Poot, A. Dadgar, N. Nan Shi, H. X. Tang, and C. Wei, OPTICS EXPRESS **20**, 26486- 26498 (2012).

[13] H H J E Kicken, P F A Alkemade, R W van der Heijden, F Karouta, R Notzel, E van der Drift and H W M Salemink, Opt. Express **17**, 22005-22011 (2009).

[14] H. H.J.E. Kicken, Ionut Barbu, Sander P. Kersten, Mehmet A. D¨undar, RobW. van der Heijden, Fouad Karouta, Richard N¨otzel, Emile van der Drift and Huub W.M. Salemink, Proc. of SPIE **7223**, 72230C-2-9 (2009).

[15] M. A. Dündar, Els C. I. Ryckebosch, R. Nötzel, F. Karouta, Leo J. van IJzendoorn, and R. W. van der Heijden, Optic Express **18** (2010).

[16] M. Loncar, A. Scherer, Microfabricated optical cavities and photonic crystals, in Optical microcavities, K Vahala ed. (World ScientificPublishing) (2004).

[17] L. Huang, H. Tian , J. Zhou, Q. Liu, P. Zhang , Y. Ji, Optics Communications **335**, 73-77 (2015).

[18] P. Zhang, H. Tian, D. Yang, Q. Liu, J. Zhou, L. Huang,Y. Ji, Optics Communications **355**, 331–336 (2015).